Journal of Thermal Analysis and Calorimetry, Vol. 66 (2001) 869–882

THERMAL EFFECTS ASSOCIATED WITH THE INCORPORATION OF TRANSITION METAL CATALYSTS INSIDE ALUMINO-SILICATE SUPPORTS

M. Riad

Egyptian Petroleum Research Institute, Nasr City, Cairo, Egypt

(Received August 13, 2000; in revised form February 26, 2001)

Abstract

Kaolinic and bentonitic-clays are selected to prepare transition metals, iron, cobalt and nickel catalysts. The metals are incorporated into two supports through new impregnation technique. The original clays and the prepared catalysts were subjected to different techniques. The crystallite size (X-ray diffraction analysis) increases from iron to cobalt then to nickel upon heating and the increase for bentonitic-catalysts is higher than that for kaolinic-ones. Infrared spectra show the appearance of bands signifying the presence of iron, cobalt and nickel bonded to OH group constituting the silica-silica tetrahedral sheets inside the clay structure. The enthalpy (ΔH) and entropy (ΔS) values (differential scanning calorimetric) are lower for bentonitic-catalysts than for kaolinic-catalysts. Thus, the incorporation of the metal hydroxide in the interlamella of the silicate-silicate bentonite clay structure facilitates the interaction between the unpaired electrons on the adjacent atoms and the support which enables the prepared catalysts to be more active for catalytic conversion.

Keywords: alumino-silicate, catalysts, clay minerals, DSC, transition metals

Introduction

The recent discovery of M41S support materials with their high surface areas and large pore volumes helps the researchers in preparing iron, cobalt and nickel transition metal catalysts. The metals in a hydroxide form were incorporated into the support at a high pH value [1]. Iron–cobalt, cobalt–nickel and nickel–iron bimetallic catalysts have been prepared using silica and titania as supports. The catalysts were prepared by the conventional incipient wetness technique. These catalysts have been used for hydrogenating carbon monoxide [2]. Zeolites have been used as support for preparing cobalt and nickel catalysts which are used in Fisher–Tropsch synthesis [3]. Zhang *et al*., [4] used sulfated alumina for preparing transition metal catalysts, meanwhile Romero *et al*., [5] used activated carbon support for preparing such catalysts. The rice husk ash supported nickel catalyst was prepared via precipitation techniques; the prepared catalyst was used for the hydrogenation of CO_2 in presence of hydrogen gas with H_2/CO_2 ratio (4/1) [6]. Sakanishi *et al*., used on iron based catalyst

1418–2874/2001/ $ 5.00

Akadémiai Kiadó, Budapest
Kluwer Academic Publishers, Dordrecht

for coal liquification process, the catalyst was prepared by impregnating the soluble iron salt into carbon nanoparticles (Ketjen black) [7].

From literature survey, it is clear that, alumina, silica, titania, zeolite, activated carbon and/or alumino-silicate were employed as support materials for preparing transition metal catalysts. In Egypt, very huge reserves of clay materials (hydrated alumino-silicate) are distributed all over the country, which encourages their use in the preparation of various types of catalysts.

The aim of this work is to study the available technique for preparing transition metal (iron-, cobalt- and nickel-) catalysts on using two different clay structures (kaolinite and bentonite) as supports. The structural phase changes that accompanying the preparation of these catalysts have been also studied.

Experimental

Preparation of catalysts

Kaolinite [from Mussabea Salama district (Sinai)] and Bentonite (from El-Hammam district (Alexandria)) clay materials have been used as supports for preparing iron-, cobalt- and nickel-catalysts.

The support-clay materials were firstly subjected to acid activation by using 2% hydrochloric acid solution in order to remove the soluble salts. Then, the monofunctional catalysts were prepared via a new impregnation technique [1]. The iron, cobalt and nickel/clay catalysts were prepared through the incorporation of the freshly prepared corresponding metal hydroxide precipitate into the two selected activated clay materials. After that, the catalysts were dried at ~150°C for 2 h, followed by calcination in presence of a stream of dry air at ~450°C for iron- and nickel-catalysts, while, at ~200°C for cobalt-catalyst.

Structural phase changes

The solid materials (supports and the prepared catalysts) were physically characterized by applying different techniques such as, X-ray analyses to study the crystalline structure and the average crystallite size using Sherrer's equation (X-ray diffraction) and to determine the constituents of the solid materials (X-ray fluorescence). Free silica is also determined [8, 9]. Infrared spectroscopic analysis has been also studied to follow the changes which occurred upon the impregnation of the transition metal cations into the silicate structures. In addition, differential scanning calorimetry was carried out to give an indication for the increase in adsorbitivity of the prepared catalysts from the enthalpy (ΔH) and the entropy (ΔS) values.

X-ray analysis

X-ray diffraction analysis was carried out using XD-D1-X-ray diffraction Shimadzu, employing a CuK_{α} radiation to study the crystalline structure and the average crystallite size for the prepared catalysts by applying Sherrer's equation [10],

$$d=\frac{K\lambda_{Cu}}{\beta_{1/2}\cos\theta}$$

where d is the average crystallite size (nm), K is the crystallite shape factor, λ_{Cu} is the wave length of CuK_{α} radiation, $\beta_{1/2}$ is the half width of the diffraction peak and θ is Bragg's angle at which the iron, cobalt and nickel peaks appear.

Infrared analysis

Infrared spectroscopic analysis was carried out using Varian Fourier transformer infrared apparatus (FTIR) [11].

Differential scanning calorimetry analysis

Differential scanning calorimetry (DSC) analysis was carried out using the differential thermal analyzer DTA-7, Perkin Elmer apparatus [12]. From the DSC charts, the enthalpy (ΔH) J g^{-1} , heat capacity (C_p) J g^{-1} °C^{-1} and the entropy (ΔS) J g^{-1} °C^{-1} were calculated [13].

The enthalpy (ΔH) is calculated by using the total area under the curve of $\Delta H/\Delta T$.

The heat capacity (C_p) is calculated from the equation:

$$C_p=\frac{\Delta H}{\Delta T},\quad \Delta T=T_2-T_1$$

where T_2 is the temperature at which the DSC peak begins to leave the base line and T_1 is the temperature at which the peak lands.

The entropy (ΔS) is calculated from the equation:

$$\Delta S=2.303C_p\log\frac{T_2}{T_1}$$

Results and discussion

Precipitation of metals hydroxide

Precipitate hydrated iron oxide 'FeO(OH)'

The hydrated iron oxide precipitate 'FeO(OH)' is prepared by adding ammonia solution drop by drop to an aqueous solution of ferric chloride salt at an ambient temperature and at a high pH value until the gelatineous brown material is formed [14].

Precipitate nickel hydroxide '$Ni(OH)_2$'

To prepare the nickel hydroxide precipitate '$Ni(OH)_2$', the sodium hydroxide solution is preferred for preparing the basic nickel as stated by Greenwood and Earnshaw [14] owing to the formation of the soluble complex salt '$[Ni(NH_3)_4(OH)_2]$' on using ammonia solution. Thus, the precipitate basic nickel '$Ni(OH)_2$' is prepared by adding

sodium hydroxide solution drop by drop to an aqueous solution of nickel chloride salt until the green precipitate of the nickel hydroxide is obtained.

Precipitate cobalt hydroxide '$Co(OH)_2$'

When ammonia solution is added drop by drop to a solution of cobalt chloride, a blue precipitate of cobalt hydroxide '$Co(OH)_2$' is obtained [14].

Preparation of transition metal-catalysts

The transition metal: 'iron-, cobalt- and nickel-catalysts' are prepared by impregnating the prepared metal hydroxides into the two clay structures (kaolinite with silica/alumina molar ratio ~2.3 'Mussabea Salama district' and bentonite with silica/alumina molar ratio ~8 'El-Hamman district').

Structural phase changes of the support and the prepared catalysts

Chemical analysis

Chemical analysis was carried out to evaluate total silica, alumina, iron and alkali metals by X-ray fluorescence and the ignition loss was determined by burning one gram sample at 1000°C till constant mass. The results of chemical analysis of raw and activated clays are presented in Table 1. The Mussabea Salama clay possesses high alumina content (~37%), low alkali content (Na_2O 1.68 and K_2O, 0.95%) as well as low percentage of (MgO, 0.77, and Fe_2O_3, 0.23%).

Table 1 Chemical analysis of raw and activated clays

Components	Mussabea Salama Clay		El-Hammam Clay	
mass%	Raw	Activated	Raw	Activated
Total SiO_2	45.84	49.8	56.91	77.79
Combined SiO_2	20.00	–	31.10	–
Free SiO_2	25.80	–	25.80	–
Al_2O_3	37.23	36.6	16.95	15.18
Na_2O	1.68	0.0	5.85	0.34
K_2O	0.95	0.0	1.32	0.0
MgO	0.77	0.0	0.87	0.0
Fe_2O_3	0.23	0.0	6.53	3.13
I.L	13.3	11.5	11.55	9.55
SiO_2/Al_2O_3	2.08	2.3	5.7	8.6

On the other hand, the chemical analysis of El-Hammam district clay shows that, it possesses low alumina content (19.95%), high percentage of iron (Fe_2O_3, 6.53%), sodium (Na_2O 5.85%) and a relatively low percentage of potassium (K_2O 1.32%).

Thus, from chemical analysis, it can be concluded that, the clay material from Mussobea salama district is mainly composed of kaolinite as reveled from the alumina content and the clay from El-Hammam district contains of sodium-bentonite as signified by the high silica/alumina ratio.

After treatment with acid, the SiO_2/Al_2O_3 molar ratio increases and the amount of alkali metals and iron becomes negligible. Loss on ignition decreases which is probably due to the fact that the clay materials may contain a larger amount of organic matter and soluble salts.

X-ray diffraction analysis for group I catalysts

X-ray diffraction patterns for the acid activated kaolinite and prepared clay catalysts (group I) are represented in Figs (1a–g).

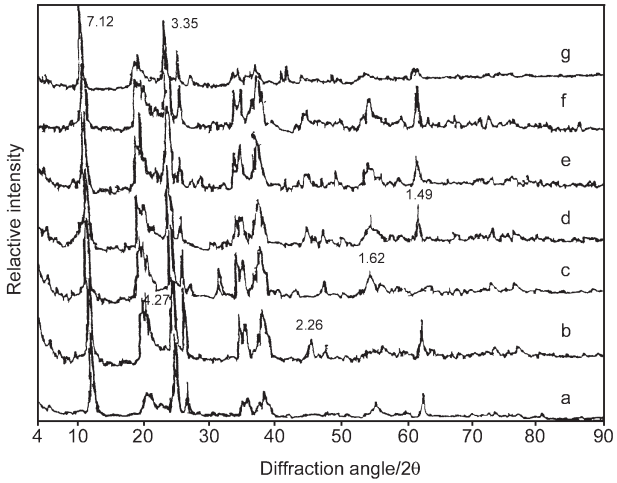

Fig. 1 X-ray diffraction patterns for group I catalysts

Diffractogram for the support clay material (Fig. 1a) reveals that, the clay material is a kaolinite as indicated by its basal reflection near 7.22, 4.27, 3.35 and 2.34 Å and it is the main constituents of this clay material, which is in accordance with chemical analyses. Quartz is also detected at *d*-spacings 3.49 and 3.37 Å.

For catalyst F-K, the X-ray diffraction pattern in Fig. (1b) indicates the presence of new reflections at *d*-spacings 4.27, 2.26 and 1.62 Å and a significant increase in some line intensities as compared with that of the support kaolinite clay (Fig. 1a). This appearance may be a result of the interaction of hydrated iron oxide species 'FeO(OH)' with the protonic acid sites of the activated kaolinite support [15]. Upon calcination of catalyst F-K (Fig. 1c), new lattice distances at *d*: 3.23, 2.75, 2.56 and 1.66 Å are created which may be related to the phase transformation of 'FeO(OH)' species to the reddish brown α-Fe_2O_3 and γ-Fe_2O_3. This is consistent with the results demonstrated by Shimada *et al*. [15].

Diffractogram for catalyst C-K (Fig. 1d) reveals the creation of new *d*-spacings at 4.27, 3.98, 1.79, 1.37 and 1.28 Å as compared with the kaolinite support. The appearance of these peaks resulted from the attack of cobalt hydroxide on the activated kaolinite clay surface. On the other hand, the diffractogram for catalyst C-K* (Fig. 1e) represents an appearance of new *d*-spacing at 3.8, 3.1, 2.99, 2.13 and 2.08 Å (as compared with catalyst C-K, Fig. 1d). This observation assumes the attack of the hydrated cobalt species and also the new formed cobalt oxide phases (CoO and CoO(OH)….ASTM 26-1107), on heating the cobalt hydroxide/clay catalyst up to 200°C.

Diffractogram for catalyst N-K also indicates the appearance of new *d*-spacings at 3.58, 3.52, 2.49, 2.20, 2.11 and 1.96 Å as compared with the support. These diffraction lines indicate the intermolecular interaction of nickel hydroxide species with the alumino-silicate structure (Fig. 1f). X-ray diffraction pattern for catalyst N-K* (Fig. 1g) represents a decrease in some line intensities as compared with catalyst (N-K), also some lattice distances appeared at 3.1, 2.29, 2.08, 1.99 and 1.49 Å. This is most probably explained in terms of the phase transformation of the nickel hydroxide species to different oxide phases, (NiO and NiO(OH),….ASTM 29-491) on heating the nickel catalyst to 450°C.

X-ray diffraction analysis for group II catalysts

The X-ray diffraction patterns for acid activated bentonite and prepared bentonite catalysts (group II) are represented in Figs (2a–g).

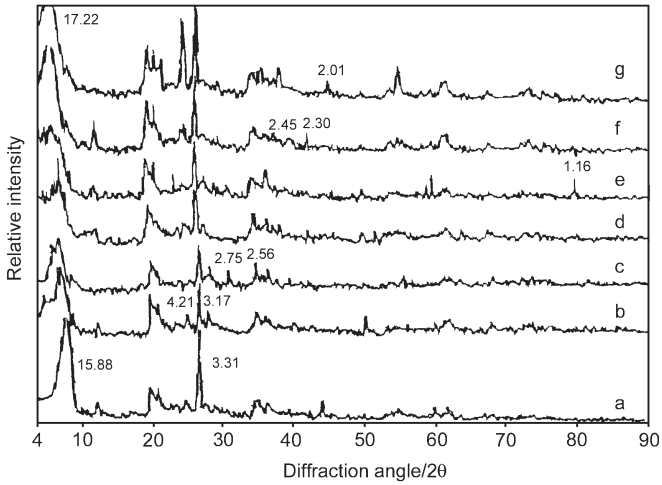

Fig. 2 X-ray diffraction patterns for group II catalysts

Diffractogram for the activated bentonite support in Fig.2a reveals that, the main characteristic lines at *d*-spacing 15.88 and 3.31 Å, indicate the support is mainly bentonite (according to ASTM cards), which is in agreement with chemical analyses.

Diffractogram for catalyst F-B (Fig. 2b) reveals an increase in some line intensities and appearance of new *d*-spacing 4.21, 4.05, 3.17 and 2.56 Å [15] (as compared with the support), which indicates the incorporation of hydrated iron oxide species into the silica-silica lamella structure of bentonite support. On heating the catalyst F-B to 450°C the hydrated iron species are transformed into the corresponding oxide species [15], as indicated from the appearance of new lattice distances at *d*-spacings: 2.75, 2.56 and 1.66 Å (Fig. 2c).

On the other hand, the X-ray diffraction pattern for catalyst C-B (Fig. 2d), reveals the appearance of new lattice distances at *d*-spacing 2.37, 1.66 and 1.29 Å which result from the incorporation of cobalt hydroxide into the silicate structure of the support. Diffractogram for catalyst C-B* (Fig. 2e) verifying the alteration of cobalt hydroxide to the corresponding oxide phases, permit the appearance of new lattice distance at *d*-spacings 2.87, 2.75, 1.56 and 1.16 Å as compared with catalyst C-B.

Diffractogram for catalyst N-B (Fig. 2f) indicates an increase in some line intensities and also creation of new lattice distances at *d*-spacing 4.05, 2.97, 2.23 and 2.11 Å. For catalyst N-B*, the diffraction patterns indicates the formation of different nickel oxide phases as noticed from the created new lines at *d*-spacings 3.98, 2.45, 2.30 and 2.01 Å (Fig. 2g).

From X-ray diffraction patterns of group I and group II catalysts, it can be concluded that, the impregnation of transition metal cations on the clay structures, results in a slight expansion within the interlayer sheets of the bentonite clay structure as evidenced by the creation of new *d*-spacings at lattice distance of 17.22 Å (Fig. 2). This has not happened in case of kaolinite type support.

Average crystallite size

The data of average crystallite size of the different impregnated cations on and/or into the two different clay structures (kaolinite and bentonite) are included in Table 2.

From these data, it is clear that, the crystallite diameter of the impregnated metals on using the kaolinite clay as support increased from 11.26 for iron to 13.2 for cobalt and then to 17.9 nm for nickel. This is because the average crystallite size is dependent on the atomic number of the metal cations. The ionic radius decreases from iron to nickel, therefore, it is easy for the smallest ionic radii (nickel) to attack and disturb the residual charge on the clay structure. This behaviour facilitates the location of such small atomic radii (nickel) either on the surface or inside the clay structure which results in an increase in the average crystallite size of the incorporated nickel cation as compared with that of the other two cations (iron and cobalt).

Concurrently, the average crystallite size for the calcined transition metal catalysts increased in the same previous sequence, i.e. increase from 14 for calcined iron catalyst to 15.6 for cobalt and then to 20.1 nm for nickel ones. The increase of the average crystallite size of cations can be explained according to the following: on heating, the cation's electron in the outer shell (unfilled orbital) absorbs energy, breaks their flow inside the atom, and then the free electrons are excited to the higher energy

level. This creates a competition between the free electrons and the strong attractive force of the nucleus, which causes an increase in the average crystallite size.

For transition metals bentonite catalysts, the incorporated hydroxide metal cations permeated through the silica-silica sheets, which also, permit the average crystallite size to increase with the decrease in the ionic radius i.e. the value of the average crystallite size for nickel is the higher one as also observed in nickel/kaolinite catalyst.

Table 2 Average crystallite size for the prepared catalysts in group I and II

Group I			Group II		
Symbol	Catalyst	Average crystallite size/nm	Symbol	Catalyst	Average crystallite size/nm
F-K	Hydrated iron oxide/kaolinite	11.26	F-B	Hydrated iron oxide/bentonite	10.94
F-K*	Hydrated iron oxide/kaolinite	14.00	F-B*	Hydrated iron oxide/bentonite	18.02
C-K	Cobalt hydroxide/ kaolinite	13.20	C-B	Cobalt hydroxide/ bentonite	19.60
C-K*	Cobalt hydroxide/ kaolinite	15.60	C-B*	Cobalt hydroxide/ bentonite	28.20
N-K	Nickel hydroxide/ kaolinite	17.90	N-B	Nickel hydroxide/ bentonite	22.50
N-K*	Nickel hydroxide/ kaolinite	20.10	N-B*	Nickel hydroxide/ bentonite	34.20

*After heat treatment

On the other hand, the values of the average crystallite size for the incorporated cations on using the bentonite as support are found to be lower than those obtained on using the kaolinite. This behaviour assured that, the hydroxide metal cations are captured in between silica-silica sheets of bentonite structure.

In an opposite way, the values of average crystallite size for the calcined transition metals/bentonite catalysts are higher than those for the calcined-kaolinite catalysts, which is probably related to the way of the rearrangement of both silica and alumina sheets to produce the two different structure supports 'kaolinite and bentonite clay structures'. Thus, upon thermal treatment, the hydroxide metal cations incorporated in between silica-silica sheets of the bentonite clay structure, may have caused the slow decomposition of the physically adsorbed water molecules [16–19] that occurred in the interlamella spacing as a result of propping the incorporated metal ion aggregates to the interlamella sheets, and result in an observed increase in the average crystallite size of the incorporated metal cations as compared with that obtained on using kaolinite clay as support for incorporating those transition metal cations.

Infrared analysis

The vibration of the atoms of clay produce a periodic displacement of the atoms with respect to one another causing a simultaneous change in interatomic distances. The infrared spectral curves of the two supports and the prepared catalysts are represented in Figs 3 and 4.

The spectrum obtained in Fig. 3a represents the appearance of the absorption bands at 473–1100 and in the range of 520–540 cm^{-1} which related to the Si–O linkage and Si–O–Al group in kaolinite respectively. Another band at 1008 cm^{-1} is due to

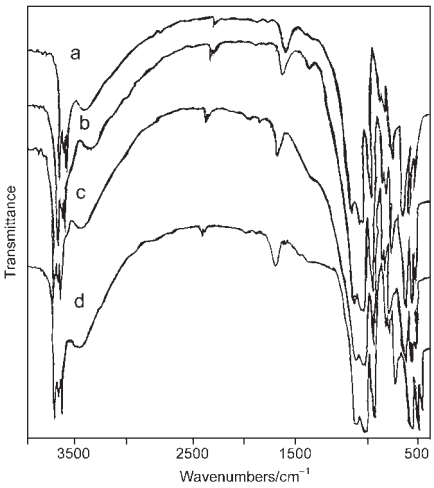

Fig. 3 Infrared spectra for group I catalysts

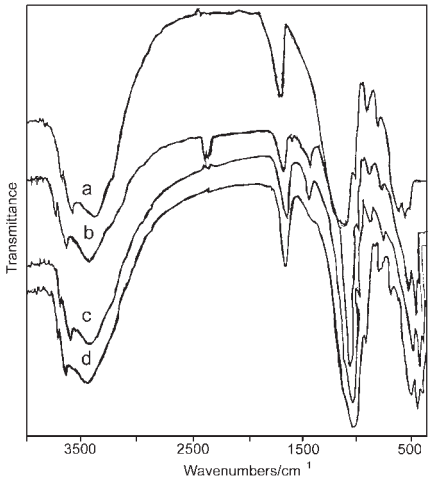

Fig. 4 Infrared spectra for group II catalysts

octahedral alumina sheet in kaolinite. Absorption bands at 915 and 1035 cm^{-1} may correspond to Al–OH group and Si–O–Si structure in bentonite (Fig. 4a).

The surface adsorbed water or hydroxyl group constituting one side of the sheet appears at 1638 cm^{-1}. The percent transmittance of this band is higher for kaolinite than for bentonite, which means that bentonite is a better adsorbent than kaolinite (Figs 3a and 4a). The absorption band which appeared in the range of 3618–3640 cm^{-1} is related to unbonded hydroxyl group between the octa- and the tetrahedral sheets of the clay structure, and that of bonded hydroxyl water inside the sheet appeared at 3695 cm^{-1}. The percent transmittance of this band is also higher for kaolinite than for bentonite. This related to the presence of lamella in between the silica-silica sheets of the bentonite clay structure, which results in an increase in its adsorption power and consequently the percent transmittance decreased. The infrared spectral analysis of the prepared transition metal hydroxide/kaolinite catalysts (group I) are represented in Figs 3b–d.

The intensity of the absorption bands of surface adsorbed water appeared at 1638 and that of the internal hydroxyl water at 3618 cm^{-1} (correspond to the Brönsted acid sites) is increased as compared with the original kaolinite bands (Fig. 3a). This increase signifies the attack of the transition metal cations Fe^{3+}, Co^{2+} and Ni^{2+} to the hydroxyl groups 'inclusive charge' in the silicate kaolinite structure as pointed from the absorption band at 916 cm^{-1} for Si–O–Fe, 696–1008 cm^{-1} for Si–O–Co and 787–1105 cm^{-1} for Si–O–Ni [20].

For transition metal cations/bentonite catalysts (group II), Figs 4b–d represent the broadening of the absorption band at 3618 cm^{-1} which confirms the incorporation of the hydroxide metal cations in between the silica-silica bentonite sheet. The intensity of this band is lower for iron catalyst than for the other two catalysts. The variation in band's intensity may be related to the ferromagnetic properties of iron, where, the existence of unpaired electrons on individual iron species delocalised and participated in the formation of a conduct band, and so, hydrogen bonding is easily formed (2458 and 2468 cm^{-1}).

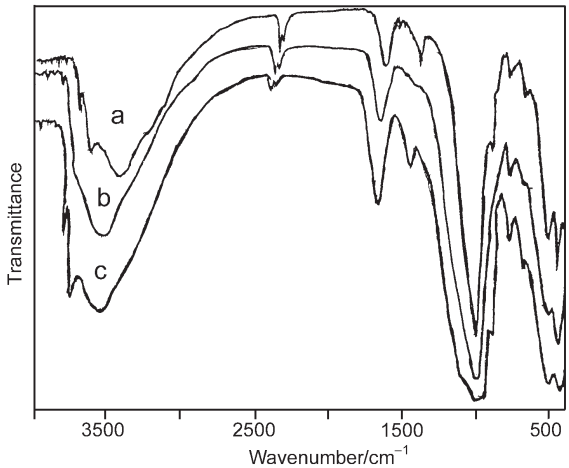

Fig. 5 Infrared spectra for iron/bentonite catalysts

Consequently, the iron cation species are more bound to the support and possess high cationic exchange on Brönsted acid sites as suggested by Mahay *et al*. [21].

Infrared spectral analysis for the heated iron/bentonite-catalysts is represented in Figs 5b and c. From the spectra, it is clear that, the percent transmittance of the absorption band at 916 cm^{-1} which is related to Si–O–Fe structure decreases from the catalyst heated at 300°C, while it increases on further increase in reaction temperature to 450°C. The intensity of absorption band at 3618 cm^{-1} related to Brönsted acid sites (internal hydroxyl group….Al–OH–Si) also showed the same behaviour i.e. the percent transmittance is higher at the elevated reaction temperature 450°C. On heating the prepared iron hydroxide/bentonite catalyst; OH stretching vibration is strongly influenced by high temperature which cause a different ionization of some water, and the Al-associated OH groups are destroyed or blocked by thermal treatment to the local dealumination [22, 23]. So, the calcination temperature 300°C is preferable to obtain iron/bentonite catalyst that possessing high Brönsted acid sites. Meanwhile, the reaction temperatures 200 and 300°C are the suitable ones for cobalt and nickel/bentonite catalysts respectively (Spectra in Figs 6a–c).

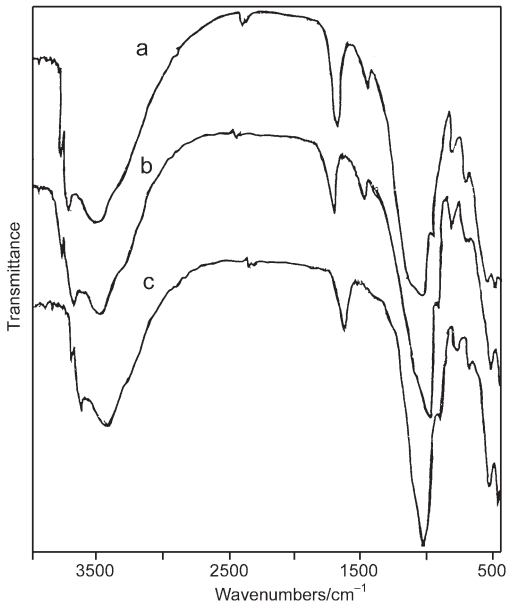

Fig. 6 Infrared spectra for heated group II catalysts

DSC

Differential scanning calorimetry data for the activated kaolinite and bentonite clay materials ‘supports’ and the prepared transition metal hydroxide catalysts are included in Table 3.

Table 3 The enthalpy 'ΔH' and the entropy 'ΔS' values for the prepared catalysts in group I and II

Catalyst	ΔH/J g^{-1}		ΔS/J g^{-1} °C^{-1}		C_p/J g^{-1} °C^{-1}	
	First endo	Second endo	First endo	Second endo	First endo	Second endo
Kaolinite	152	605.8	2.19	1.12	1.35	1.44
F-K	152.4	538.5	2.21	1.01	1.64	2.11
C-K	183.0	554.2	2.58	1.02	1.44	2.45
N-K	180.7	541.2	2.67	1.01	1.52	2.31
Bentonite	412.8	151.2	5.79	0.34	3.17	0.69
F-B	374.8	104.2	4.54	0.220	2.58	0.65
C-B	311.6	114.8	6.02	0.217	2.59	0.74
N-B	402.1	108.9	4.54	0.243	3.49	0.66

Differential thermal profiles for the acid-activated clays exhibit two endothermic peaks and one exothermic peak. The first endothermic peak, in the temperature range 100–160°C, indicates the evolution of physically adsorbed water and also the surface water of the clays. The second endothermic peak, in the temperature range 500–550°C, is caused mainly by the loss of the structural water in agreement with several publishers [16–19]. However, the exothermic peak is a structural one and is actually attributed to the destruction of clay structures and the formation of new phases.

Upon the inclusion of cobalt and nickel on acid-activated kaolinite, (group I catalysts), the enthalpy values (ΔH=heat content of catalysts) are sharply influenced. The enthalpy values for the first surface adsorption peak increased from 152 J g^{-1} for the mother kaolinite to 152.4, 183 and 180.7 J g^{-1} for iron-, cobalt- and nickel-catalysts respectively (Table 3). The increase in the enthalpy value is probably related to that, the dehydration depends on the ionic charge of the exchanged cations i.e. as the ionic charge increases, the dehydration temperature increases [24]. Thus, Fe-, Co- and Ni- are considerably more resistant to dehydration than sodium-clay (in mother clay material). On the other hand, the entropy values (ΔS) are also influenced in the same way (Table 3).

For the second endothermic peaks, the enthalpy values 'ΔH' decreased from 605.8 for the support to 538.5, 554.2 and 541.2 J g^{-1} for iron-, cobalt- and nickel-catalysts respectively. The reduction in 'ΔH' values is an indication of the strong inclusion of the metal species on the clay surface framework structure, i.e. no hydroxyl groups are free. This observation is in parallel with the data obtained from X-ray diffraction which provides the creation of new *d*-spacing at lattice distance of 2.26, 1.62 Å for iron-, 3.98, 1.37 Å for cobalt- and 2.96, 2.1 Å for nickel-catalysts.

For catalysts in group II, the enthalpy values for the first endothermic peaks (Table 3) are high than that for catalysts in group I. This may be related to the high adsorption power efficiency of bentonite clay over kaolinite (owing to its lamella structure). Meanwhile, the enthalpy values for the second endothermic peaks are low as compared with that for group I. These changes are related to that, bentonite is known to contain less

structural water than kaolinite and also to confirm the incorporation of metal cation species inside the silica-silica lamella sheets in the bentonite clay structure.

Thus, the presence of different cations (iron, cobalt and nickel) of varying hydration capacities between the silicate layers structure of bentonite may bear some contribution to the sorbed water. The dehydration process becomes easier and consequently the enthalpy values decrease with the incorporation of metal ions. On the other hand, the highest values of the entropy 'ΔS' for the first endothermic peak for catalysts in group II, may also relate to the system disordering resulting from the highest adsorption power of bentonite (Table 3).

From the previous results, it can be concluded that, the values of enthalpy 'ΔH', for the second endothermic peaks for catalysts in group I and II decreasing in the sequence; iron<nickel<cobalt.

The lowest enthalpy values for iron catalysts are related to the highest ferromagnetic character of the iron cation species as compared with the other two species 'nickel and cobalt which are more bound inside the silicate structure'.

Conclusions

Iron, cobalt and nickel/clays catalysts are prepared by a new impregnation technique on using the kaolinic and bentonitic clays as supports. The metals are incorporated into the silicate clay structure in the form of metal hydroxide to ensure the metal cations to be bound on and inside the silicate framework structures.

The prepared catalysts are physically characterized by applying different techniques such as; X-ray analyses to study the crystalline structure and the average crystallite size using Sherrer's equation (X-ray diffraction), and to determine the constituents of the solid materials (X-ray fluorescence). Infrared spectroscopic analysis is also studied to follow the changes occurred upon the impregnation of the transition metal cations into the silicate structures. In addition, differential scanning calorimetry analysis is carried out to give an indication for the increase in adsorptivity of the prepared catalysts from the enthalpy 'ΔH' and entropy 'ΔS' values.

X-ray diffraction established that, the average crystallite size increased with the increase in the atomic number, i.e. with the decrease in the ionic radius form iron to cobalt then to nickel. The rearrangement of silica and alumina sheets has a pronounced effect on the crystallite size values.

Infrared spectral analysis confirms the bonding of iron, cobalt and nickel to OH group constituting the silica-silica tetrahedral and the silica-alumina octahedral sheets on and inside the clay structure. On heating the catalysts, the intensity of the absorption band at 3618 cm^{-1} corresponding to the Brönsted acid sites increases at 300°C for the iron and nickel catalysts and at 200°C for cobalt catalyst.

The enthalpy and entropy values calculated from differential scanning calorimetry are lower for bentonite and bentonite catalysts than those obtained for kaolinite and kaolinite catalysts. This relates to the presence of the weak parallel lamella region of the silica-silica sheets of the bentonitic clay structure (as compared with the

corresponding kaolinite one). This confirms that dehydration processes does not need high absorbed heat and the incorporation and the capture of the metals is much easier.

* * *

Financial support provided by Prof. Dr. Sara Mikhail, Head of Catalysis Laboratory Refining Department (EPRI) is gratefully acknowledged, thanks for her valuable and helpful suggestions and fruitful discussion during this work.

References

1 J. L. Epperlein, J. G. Moore and C. C. Landry, 215th National Meeting, American Chemical Society, Dallas, TX, March 29–April 3, 1998, 315.
2 T. Ishihara, K. Eguchi and H. Arai, Applied Catalysts, 30 (1987) 225.
3 D. J. Koh, J. S. Chung and Y. G. Kim, Ind. Eng. Chem. Res., 34 (1995) 1969.
4 Q. Zhang, M. Kantcheva and I. G. D. Lana, Ind. Eng. Chem. Res., 36 (1997) 3433.
5 M. D. Romero, J. A. Calles and A. Rodriguez, Ind. Eng. Chem. Res., 36 (1997) 3533.
6 F. W. Chang, T. J. Hsiao and J. D. Shih, Ind. Eng. Chem. Res., 37 (1998) 3838.
7 K. Sakanishi, H. Taniguchi, H. Hasuo and I. Mochida, Ind. Eng. Chem. Res., 36 (1997) 306.
8 G. R. Rigby, The Thin-Section Mineralogy of Ceramic Materials, Brit. Refr. Res. Ass., 1948.
9 S. Mikhail, N. Rizk, B. Girgis and I. K. Abdou, Revue de l'Institut Français du Pétrole, 26 (1971) 1077.
10 L. N. Shell and S. Bhatla, Ind. Eng. Chem. Res., 25 (1986) 530.
11 V. Venugopal, J. Therm. Anal. Cal., 60 (2000) 107.
12 M. Kristofic, A. Marcincin and A. Ujhelyiova, J. Therm. Anal. Cal., 60 (2000) 357.
13 J. A. Campell, Chemical Systems Energetics, Dynamics, Structure, W. H. F. Freeman and Co., San Francisco 1970.
14 N. N. Greenwood and A. Earnshaw, Chemistry of Elements, Pergamon Press, Oxford 1984.
15 T. Shimada, T. Kajinami, T. Kumagai, S. Takeda, J. I. Hayashi and T. Chiba, Ind. Eng. Chem. Res., 37 (1998) 894.
16 G. R. Grim, Applied Clay Mineralogy, McGraw Hill, 1962.
17 S. Mikhail, S. M. Ayoub and Y. Barakat, Zeolites, 7 (1987) 231.
18 S. Mikhail, Y. Barakat and A. El-Naggar, Egypt. J. Petrol., 3 (1994) 17.
19 S. Mikhail, A. El-Bassoussy and M. Kh. Tannous, Egypt. J. Petrol., 4 (1995) 11.
20 K. Iwai and H. Samo, J. Catalysis, 106 (1987) 428.
21 A. Mahay, F. Semard, G. Lemay, A. Adnot, S. Kaliaguine and J. Monnier, Applied Catalysts, 33 (1971) 55.
22 J. C. Vedrine, A. Auroux, G. Coudurier, P. Engellard, J. P. Galles and G. Szabo, Proc. 6th Intern. Zeol. Conf., Remo/Nevada, 1983, p. 466.
23 U. Kursehner, B. Parlitz, E. Schreier, G. Ohlmann and J. Volter, Appl. Catalysis, 30 (1987) 159.
24 S. Mikhail, Study on the Isomerization of *n*-paraffins over Synthetic Zeolites Ph. D. Thesis, Faculty of Science, Mansoura University 1978.